Evaluation of RCS Measurement Environment in Compact Anechoic Chamber

Naobumi Michishita, Tadashi Chisaka, and Yoshihide Yamada
National Defense Academy
1-10-20 Hashirimizu
Yokosuka, 239-8686 JAPAN

***Abstract*- To enhance the dynamic range of monostatic RCS measurement in compact anechoic chamber, this paper presents the quantitative evaluation of simple CW measurement method by using transmitting and receiving antennas. The mutual coupling is reduced by several approaches such as the separation between antennas, suppressing the sidelobe level, and inserting the shielded conductor. The measurable maximum and minimum RCS values are clarified. The effect of the arrangement of wave absorber in target side is also shown.**

I. Introduction

Recently, the monostatic RCS of a patch antenna with different terminal loads has been investigated [1]-[3]. We have verified a RCS reduction of 15 dB by applying high resistive load of 500Ω through both simulation and measurement [4]. In the monostatic RCS measurement of the patch antenna with resistive load, the minimum RCS value becomes about −30 dBsm. To measure the low receiving level, the arrangement of transmitting and receiving antennas and the appropriate employment of wave absorbers are important. In this paper, the effect of RCS measurement environment in compact anechoic chamber is estimated quantitatively by electromagnetic simulation. Typical RCS measurement techniques are the continuous wave (CW) method by using simple transmitting and receiving antennas, and the pulsed measurement method by using time domain function in the network analyzer. To evaluate the simplified RCS measurement method, the CW method is employed in this paper.

II. Major Factor of Mutual Coupling Between Transmitting and Receiving Horns

The major factor of mutual coupling between transmitting and receiving horn antennas is investigated. Figure 1 shows the measurement environment for monostatic RCS of a patch antenna with resistive load in compact anechoic chamber. The mutual coupling derived from Friss formula is given by

$$\frac{P_r}{P_t} = G_t(\theta = 90°)G_r(\theta = 90°)L(d) \qquad (1)$$

where P_t and P_r are transmitting and receiving power, G_t and G_r are transmitting and receiving antenna gain, d is the distance between antennas, and $L(d) = (\lambda / 4\pi d)^2$ is free space path loss. Figure 2(a) shows the configuration of the transmitting and receiving horns. In this paper, horizontal polarization is employed. Figure 2(b) shows the radiation

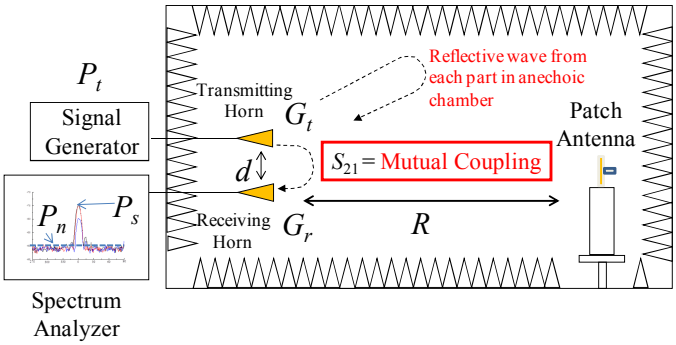

Figure 1. Measurement environment for monostatic RCS of patch antenna with resistive load in anechoic chamber.

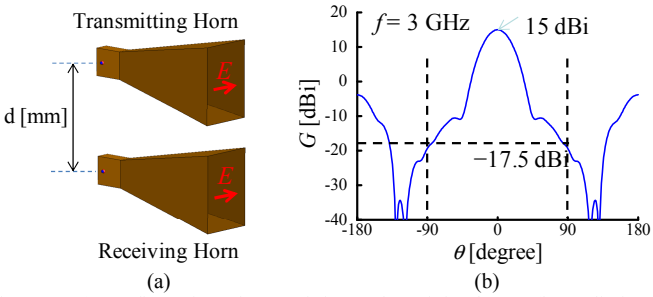

Figure 2. (a) Configuration of transmitting and receiving horns. (b) Radiation pattern of horn antenna

TABLE I
Mutual Coupling Between Transmitting and Receiving Horns and Simulated S21

d	$G_t + G_r$	$L(d)$	P_r/P_t	S_{21}
300 mm	−35 dB	−31.5 dB	−66.5 dB	−67.0 dB
600 mm		−37.5 dB	−72.5 dB	−71.8 dB
900 mm		−41.0 dB	−76.0 dB	−76.1 dB

pattern of the horn antenna at 3 GHz. The simulated results are obtained by moment method. The antenna gain is 15 dBi and the sidelobe level at θ = 90 deg. is −17.5 dBi. Table I shows the mutual coupling between horns when d is varied. Since transmitting and receiving horns are identical, G_t + G_r becomes −35 dB. Table I also shows S_{21} obtained by electromagnetic simulation. The mutual coupling calculated by Eq. (1) and simulated S_{21} are almost identical. Figure 3 shows S_{21} characteristics when d is varied. S_{21} of −100 dB can be achieved with d = 14 m. Therefore, The reduction of G_t + G_r or $L(d)$ are required for mutual coupling suppression.

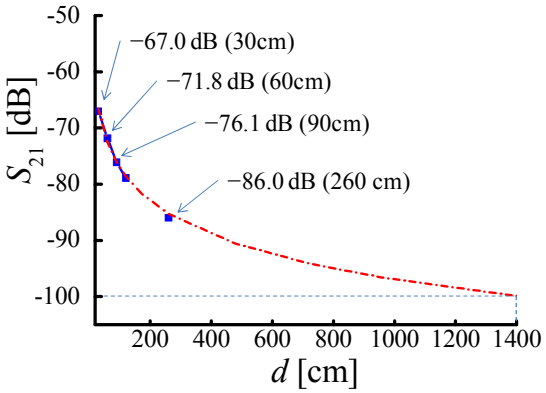

Figure 3. S_{21} characteristics when distance d between horns is varied.

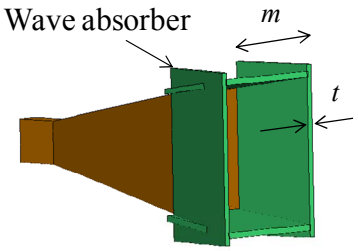

Figure 4. Horn antenna with wave absorber for reduction of sidelobe level.

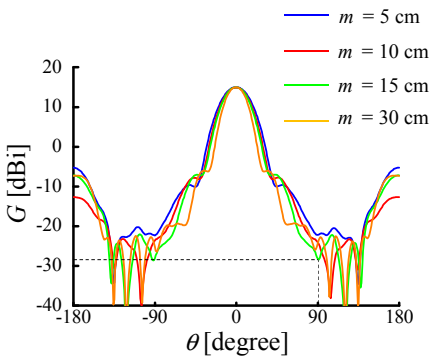

Figure 5. Radiation pattern of horn antenna with t = 1 cm when m is varied.

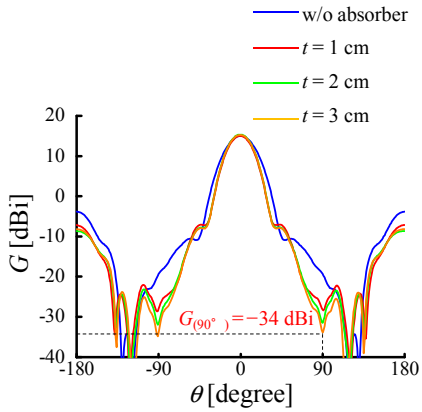

Figure 6. Radiation pattern of horn antenna with m = 15 cm when t is varied.

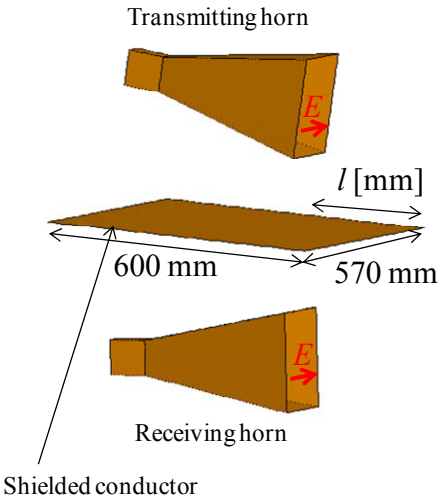

Figure 7. Configuration of shielded conductor inserted between horns.

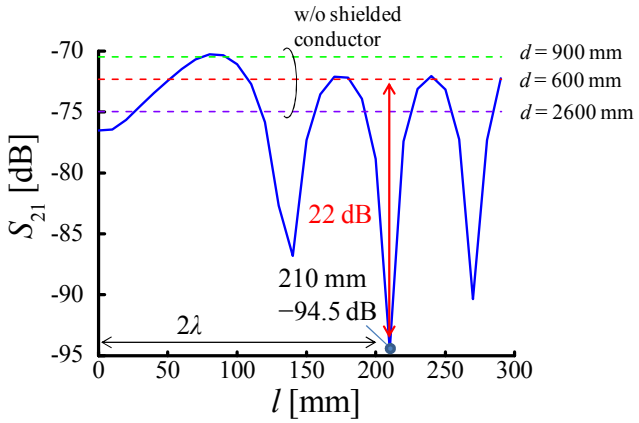

Figure 8. S_{21} characteristics when l is varied.

III. Mutual Coupling Reduction Techniques

First, the arrangement of wave absorber is examined for reduction of sidelobe level to reduce $G_t + G_r$. Figure 4 shows the configuration of horn antenna with wave absorber. The wave absorber is arranged at the edge of the horn antenna. Figure 5 shows the radiation pattern with t = 1 cm when m is varied. The sidelobe level at θ = 90 deg. can be suppressed at m = 15 cm. Figure 6 shows the radiation pattern with m = 15 cm when t is varied. The sidelobe level at θ = 90 deg. becomes −34 dBi at t = 3 cm.

Next, the arrangement of shielded conductor is examined for reduction of path loss to reduce $L(d)$. Figure 7 shows the configuration of shielded conductor inserted between horns. The position of the shielded conductor is middle of two antennas. Figure 8 shows S_{21} characteristics when l is varied. The mutual coupling reduction of 22 dB is achieved with l = 2λ due to standing wave occurred by diffraction at shielded conductor.

TABLE II
MUTUAL COUPLING REDUCTION EFFECTS

Method	$G_t + G_r$	$L(d)$	P_r/P_t	S_{21}
Horn only	−35 dB	−37.5 dB	−72.5 dB	−72.3 dB
Sidelobe reduction	−68 dB	−37.5 dB	−105.5 dB	−78.0 dB
Shielded conductor	−35 dB	−59.5 dB	−94.5 dB	−94.5 dB

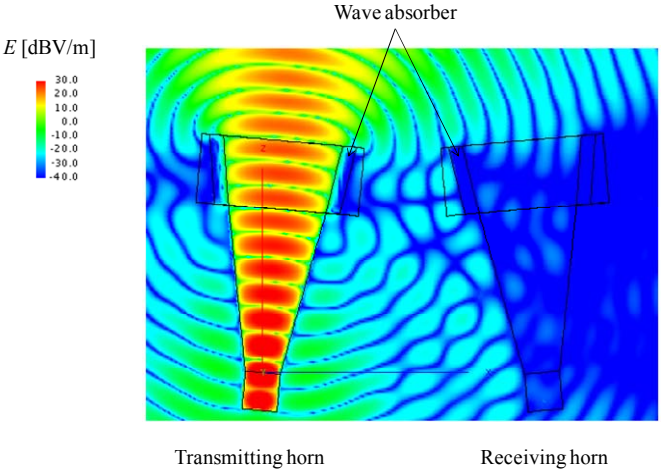

Figure 9. Near field distribution of two horn antennas with wave absorber.

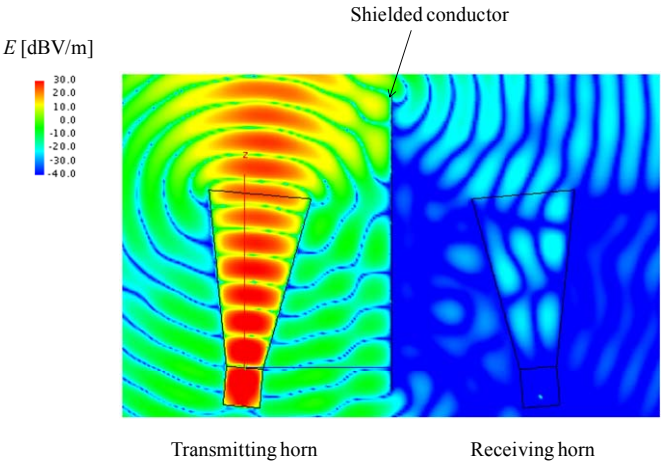

Figure 10. Near field distribution of two horn antennas with shielded conductor.

Table II shows the mutual coupling reduction effect. In the case of the sidelobe reduction method, the mutual coupling calculated from Eq. (1) is −105.5 dB, which is not identical to the simulated S_{21} of −78.0 dB. In the case of the shielded conductor method, both P_r/P_t and S_{21} agree well.

Figures 9 show the near field distribution of two horn antennas with wave absorber. The discrepancy of P_r/P_t and S_{21} seems to be due to approaching each aperture planes by adding wave absorber. Figures 10 show the near field distribution of two horn antennas with shielded conductor. Although strong electric field intensity is confirmed inside horn antenna, the feed position becomes standing wave node.

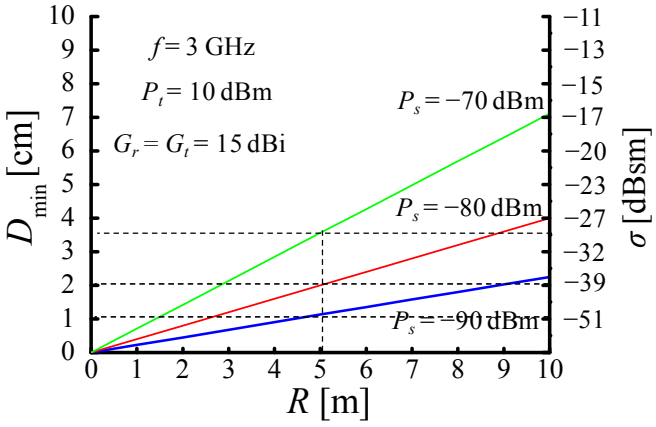

Figure 11. Measurable minimum RCS values.

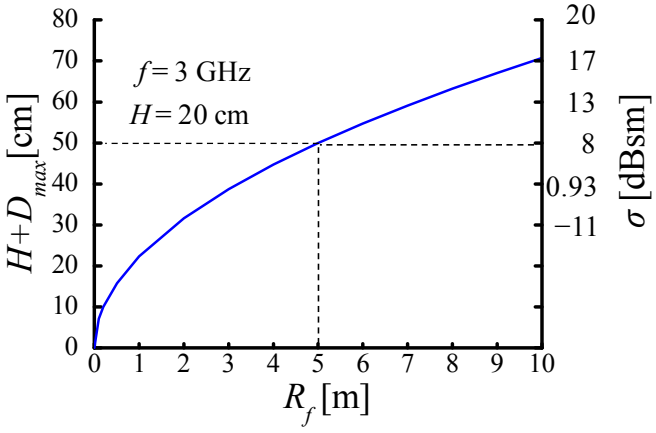

Figure 12. Measurable maximum RCS values.

IV. MEASURABLE MAXIMUM AND MINIMUM RCS VALUES

The minimum S_{21} of −94.5 dB estimated in previous section corresponds to the receiving power P_r = −84.5 dBm when transmitting power P_t = 10 dBm. The radar equation is given by

$$P_r = P_t G_t G_r \left(\frac{D}{4R}\right)^4 \tag{2}$$

where D is the target size, and R is distance between horns and target. Figure 11 shows the measurable minimum RCS values. σ is the theoretical RCS value of D of the circular disk. The measurable minimum RCS value is −40 dBsm with R = 5 m and Pr = −84.5 dBm at 3 GHz. Figure 12 shows the measurable maximum RCS values. The far field condition is given by

$$H + D_{max} = \sqrt{R_f / 20} \tag{3}$$

where H is the aperture size of horn, and D_{max} is the measurable maximum target size. The measurable maximum RCS value and D_{max} are 8 dBsm and 30 cm with R_f = 5 m and H = 20 cm.

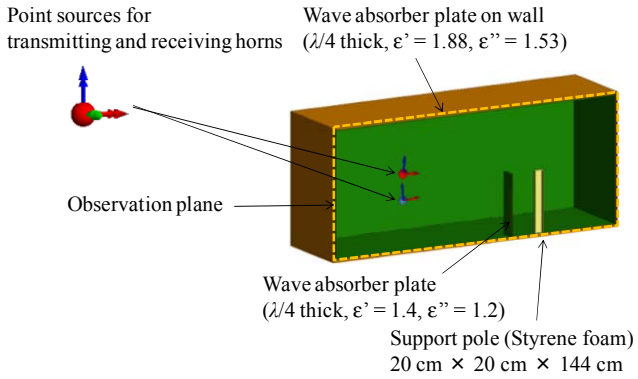

Figure 13. Configuration of anechoic chamber.

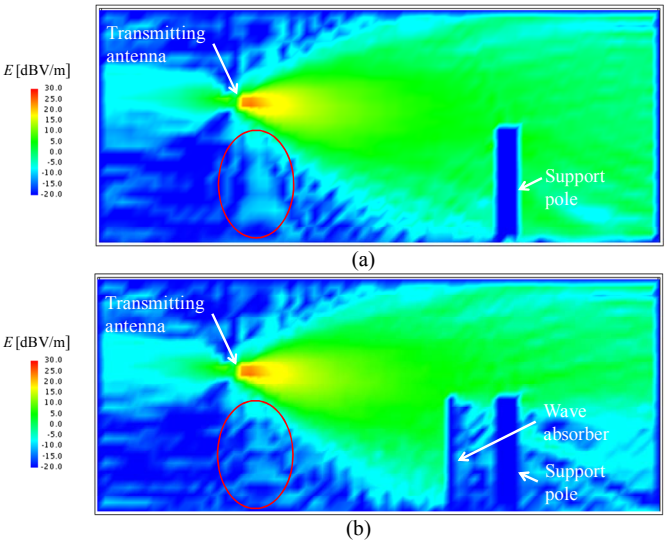

Figure 14. Electric field distributions at observation plane (a) with support pole and (b) wave absorber plate placed in front of support pole.

TABLE III
MUTUAL COUPLING REDUCTION EFFECTS IN SEVERAL ENVIRONMENT CONDITIONS

Conditions	P_r/P_t
Free space	−73.6 dB
In anechoic chamber	−71.6 dB
Existing support pole	−59.6 dB
Put wave absorber	−64.4 dB

V. GO SIMULATION IN ANECHOIC CHAMBER

Figure 13 shows the configuration of anechoic chamber. The effects of the measurement environment are estimated thorough GO simulation. The length, width, and height of the compact anechoic chamber are 7 m × 3.705 m × 2.915 m. In GO simulation, the far field radiation patterns of the horn antenna are employed as point sources at the transmitting and receiving horns. And, the number of reflection/transmission interactions for each ray is 3. Typical pyramidal wave absorber put on the wall in compact anechoic chamber is modeled as the single layer of the dielectric material with λ/4 thick. The reflection reduction of this dielectric sheet is 59 dB in oblique incidence of 45°. There are support pole composed of styrene foam and the wave absorber for normal incidence in the target side.

Figure 14 shows the electric field distributions at longitudinal plane at center of the anechoic chamber with the support pole and the wave absorber plate placed in front of the support pole. The electric field intensities at receiving area are affected by the support pole and wave absorber. Table III shows the mutual coupling reduction effect in several environment conditions. The existing of the support pole increases the mutual coupling of 12.0 dB. The reflection from the support pole can be reduced by placing the wave absorber in front of the support pole.

VI. CONCLUSION

This paper presents the evaluation of the RCS measurement environment in compact anechoic chamber. The electromagnetic simulation results help us to achieve the mutual coupling reduction of the transmitting and receiving horns. Further improvement of the measurable minimum RCS values is also important to measure the lower RCS values in future.

REFERENCES

[1] Y. Liu, S.-X. Gong, and D.-M. Fu, "A novel model for analyzing the RCS of microstrip antenna," *IEEE AP-S Int. Symp.*, Columbus, OH, vol.4, pp.835-838, June 2003.

[2] D.M. Pozar, "Radiation and scattering from a microstrip patch on a uniaxial substrate," *IEEE Trans. Antennas Propagat.*, vol.35, no.6, pp.613-621, June 1987.

[3] Y. Inasawa, Y. Nishioka, N. Yoneda, and Y. Konishi, "Radar Cross Section Analysis of a Patch Antennas Considering Terminal Conditions," *IEICE Communications Society Conference*, C-1-4, Sep. 2011 (in Japanese).

[4] T. Chisaka, N. Michishita, and Y. Yamada, "Reduction of RCS Values of a Patch Antenna by Resistive Loading," *IEEE AP-S Int'l Symp.*, Orlando, FL, July 2013.